k-ϵ Model for the Atmospheric Boundary Layer Under Various Thermal Stratifications

Cédric Alinot
Ph.D. student

Christian Masson[1]
Professor
e-mail: christian.masson@etsmtl.ca

École de Technologie Supérieure,
Department of Mechanical Engineering,
Montréal, QC H3C 1K3 Canada

This paper presents a numerical method for predicting the atmospheric boundary layer under stable, neutral, or unstable thermal stratifications. The flow field is described by the Reynolds' averaged Navier-Stokes equations complemented by the k-ϵ turbulence model. Density variations are introduced into the momentum equation using the Boussinesq approximation, and appropriate buoyancy terms are included in the k and ϵ equations. An original expression for the closure coefficient related to the buoyancy production term is proposed in order to improve the accuracy of the simulations. The resulting mathematical model has been implemented in FLUENT. *The results presented in this paper include comparisons with respect to the Monin-Obukhov similarity theory, measurements, and earlier numerical solutions based on k-ϵ turbulence models available in the literature. It is shown that the proposed version of the k-ϵ model significantly improves the accuracy of the simulations for the stable atmospheric boundary layer. In neutral and unstable thermal stratifications, it is shown that the version of the k-ϵ models available in the literature also produce accurate simulations.* [DOI: 10.1115/1.2035704]

1 Introduction

This paper was motivated by the goal of quantifying the effects of atmospheric boundary layer thermal stratification on wind-turbine and wind-park performances. The first task towards reaching this goal is to make an adequate, efficient prediction of the atmospheric boundary layer under various conditions of thermal stratification. This is the main subject of this paper, where a mathematical model capable of handling the atmospheric boundary layer under various thermal stratifications is proposed and implemented in FLUENT.

The flow field in a wind park immersed in the atmospheric boundary layer can be described by the Reynolds' averaged incompressible three-dimensional Navier-Stokes equations. Atmospheric, wake shear-generated and blade-generated (viscous and pressure effects due to the blades) turbulence are the three major contributors to the turbulence in the wake of a wind turbine and within a wind park. Various experiments have demonstrated that in the first two diameters downstream of a rotor, strong turbulence is generated by the degradation of tip vortices and by shear production [1,2]. Further downstream, turbulence properties recover their upstream values and thus, atmospheric turbulence controls the growth of the wake. Therefore, a model taking both shear-generated and atmospheric turbulence into account is a minimum requirement. Two equation turbulence models meet this requirement. The modified k-ϵ model for shear flow under gravitational influence [3] has been chosen for the closure of the Reynolds' averaged, turbulent flow equations, mainly because of its wide use and because of the availability of k and ϵ properties of the atmospheric boundary layer in meteorological data [4]. This turbulence model has been applied to neutral atmospheric boundary layer by Crespo et al. [5] to study wind turbine wake characterictics and more recently by Riddle et al. [6] to simulate atmospheric dispersion.

The main object of this paper is to improve the accuracy of the k-ϵ model when applied to the atmospheric boundary layer under various conditions of thermal stratification. Thanh et al. [7] and Apsley and Castro [8] have also implemented a k-ϵ model for various atmospheric stability. It is important to note that standard mesoscale meteorological CFD models traditionally use higher-order turbulence models [9].

2 Formulation

In this paper, the flow of interest is the one observed in the first hundred meters of the atmospheric boundary layer, over uniform flat terrain under various thermal stratification conditions (stable, neutral, or unstable). Consequently, the Coriolis acceleration can be neglected, and it can be assumed that the fluid is incompressible and the flow steady. The Cartesian coordinate system is used in this paper with z being the vertical coordinate (z=0 at the ground), x being parallel to the ground and in the direction of the flow, and y being parallel to the ground and perpendicular to the flow direction.

2.1 Governing Equations. For steady and incompressible flow conditions, the Reynolds' averaged Navier-Stokes equations in tensor form notation can be written as

$$\int_{\mathcal{A}} u_i n_i d\mathcal{A} = 0 \tag{1}$$

$$\int_{\mathcal{A}} \rho u_j u_i n_i d\mathcal{A} = -\int_{\mathcal{A}} p\delta_{ij} n_i d\mathcal{A} + \int_{\mathcal{A}} \tau_{ij} n_i d\mathcal{A} + \int_{\mathcal{V}} \rho g_j d\mathcal{V} \tag{2}$$

$$\int_{\mathcal{A}} \rho c_p T u_i n_i d\mathcal{A} = \int_{V} \rho u_i g_i d\mathcal{V} + \int_{\mathcal{A}} \left[u_j \tau_{ij} + \frac{c_p \mu_t}{\sigma_T} \left(\frac{\partial T}{\partial x_i} - \frac{g_i}{c_p} \right) \right] n_i d\mathcal{A} \tag{3}$$

where $\mathcal{A}$ denotes an outer surface of fixed volume $\mathcal{V}$, u_i is the i_{th} flow velocity component, n_i is the appropriate cosine director of the outward unit vector $\mathbf{n}$ perpendicular to the elementary control surface $d\mathcal{A}$, ρ is the fluid density, p is the pressure, δ_{ij} is the Kronecker delta, τ_{ij} is the viscous-stress tensor (which includes

[1]Correspondence to: Christian Masson, École de Technologie Supérieure, 1100 Notre-Dame Ouest, Montréal, Québec, Canada, H3C 1K3. Telephone: (514) 396-8504; fax: (514) 396-8530; e-mail: christian.masson@etsmtl.ca. Holder of the Canada Research Chair in the Aerodynamics of Wind Turbines in Nordic Environment.

Contributed by the Solar Energy Division of THE AMERICAN SOCIETY OF MECHANICAL ENGINEERS. Manuscript receieved by the ASME Solar Division November 19, 2004; final revision May 26, 2005. Associate editor: D. Berg.

the Reynolds stress tensor), g_i is the i_{th} component of gravitational acceleration, c_p is the dry air specific heat at constant pressure, T is the temperature, μ_t is the turbulent viscosity, and σ_T is the turbulent Prandtl number. The Boussinesq approximation is used: The density ρ is assumed to vary linearly with temperature only in the gravity term. It is important to note that the summation convention applies to Eqs. (1)–(3).

2.2 Turbulence Modeling of the Flow. For a control volume $\mathcal{V}$ delimited by an outer surface $\mathcal{A}$, standard equations for the k-ϵ model [10,11] are:

$$\int_{\mathcal{A}} \rho k u_i n_i d\mathcal{A} = \int_{\mathcal{V}} [P_t - \rho\epsilon + G_b] d\mathcal{V} + \int_{\mathcal{A}} \frac{\mu_t}{\sigma_k} \frac{\partial k}{\partial x_i} n_i d\mathcal{A} \tag{4}$$

$$\int_{\mathcal{A}} \rho \epsilon u_i n_i d\mathcal{A} = \int_{\mathcal{A}} \frac{\mu_t}{\sigma_\epsilon} \frac{\partial \epsilon}{\partial x_i} n_i d\mathcal{A} + \int_{\mathcal{V}} \left[C_{\epsilon 1} \frac{\epsilon}{k} (P_t + (1 - C_{\epsilon 3}) G_b) - C_{\epsilon 2} \rho \frac{\epsilon^2}{k} \right] d\mathcal{V} \tag{5}$$

$$P_t = \mu_t \left(\frac{\partial u_i}{\partial x_j} + \frac{\partial u_j}{\partial x_i} \right) \frac{\partial u_i}{\partial x_j} \tag{6}$$

$$G_b = \beta g_i \frac{\mu_t}{\sigma_T} \left(\frac{\partial T}{\partial x_i} - \frac{g_i}{c_p} \right) \tag{7}$$

$$\mu_t = \rho C_\mu \frac{k^2}{\epsilon} \tag{8}$$

β is the air thermal volumetric expansion coefficient. G_b and P_t are the production (or removal) of turbulent kinetic energy by buoyancy forces and shear, respectively. The term g_i/c_p is the dry adiabatic lapse rate. When the vertical temperature gradient $\partial T/\partial z$ is larger than the dry adiabatic lapse rate, the atmospheric boundary layer is in unstable thermal stratification and G_b is positive. On the other end, when the vertical temperature gradient $\partial T/\partial z$ is smaller than the dry adiabatic lapse rate, G_b is negative and this corresponds to a stable thermal stratification.

In the original model proposed by Jones and Launder [10], G_b=0 and the values for the closure coefficients are:

$$C_{\epsilon 1} = 1.44 \quad C_{\epsilon 2} = 1.92 \quad C_{\epsilon 3} = 1.0$$
$$C_\mu = 0.09 \quad \sigma_k = 1.0 \quad \sigma_\epsilon = 1.3 \tag{9}$$

2.3 Description of the Basic Flow. The expressions describing the atmospheric flow over uniform flat terrain are based on the Monin-Obukhov similarity theory and have been taken from Panofsky and Dutton [4].

The turbulent viscosity is expressed by the mixing length relation:

$$\mu_{t0}(z) = \frac{\rho K u_* z}{\phi_m\left(\frac{z}{L}\right)} \tag{10}$$

where K is the von Karman constant (K=0.42), z the vertical coordinate (z=0 at the ground), L the Monin-Obukhov length, and ϕ_m the nondimensional wind shear. The Monin-Obukhov length is an estimate of the height where G_b is comparable with P_t [8]. Using the Reynolds' analogy, turbulent heat diffusivity is related to turbulent viscosity through a turbulent Prandlt number [4]:

$$\sigma_T = 1 \tag{11}$$

The Monin-Obukhov length and the nondimensional wind shear are expressed by the following relations [4]:

$$L = \frac{u_*^2 T_w}{K g T_*} \tag{12}$$

$$\phi_m\left(\frac{z}{L}\right) = \begin{cases} \left(1 - 16\frac{z}{L}\right)^{-\frac{1}{4}} & L < 0 \\ 1 + 5\frac{z}{L} & L > 0 \end{cases} \tag{13}$$

The turbulent friction velocity u_* and temperature T_* are expressed by:

$$u_* = \sqrt{\frac{\tau_w}{\rho}} \tag{14}$$

$$T_* = \frac{-\dot{q}_w}{\rho c_p u_*} \tag{15}$$

where τ_w is the surface shear stress, T_w the surface temperature, $\dot{q}_w$ the surface heat flux, and g the gravitational acceleration module.

Assuming the shear stress and heat flux to be constant over the lower part of the atmospheric boundary layer, modified logarithmic velocity and temperature profiles are obtained [4]:

$$u_0(z) = \begin{cases} \frac{u_*}{K}\left[\ln\left(\frac{z}{z_0}\right) + \ln\left(\frac{8\phi_m^4\left(\frac{z}{L}\right)}{\left(\phi_m\left(\frac{z}{L}\right)+1\right)^2\left(\phi_m^2\left(\frac{z}{L}\right)+1\right)} \right) - \frac{\pi}{2} + 2\arctan\left(\frac{1}{\phi_m\left(\frac{z}{L}\right)} \right) \right] & L < 0 \\ \frac{u_*}{K}\left[\ln\left(\frac{z}{z_0}\right) + \phi_m\left(\frac{z}{L}\right) - 1 \right] & L > 0 \end{cases} \tag{16}$$

$$T_0(z) - T_w = \begin{cases} \frac{T_*}{K}\left[\ln\left(\frac{z}{z_0}\right) - 2\ln\left[\frac{1}{2}\left(1 + \phi_m^{-2}\left(\frac{z}{L}\right)\right)\right]\right] - \frac{g}{c_p}(z - z_0) & L < 0 \\ \frac{T_*}{K}\left[\ln\left(\frac{z}{z_0}\right) + \phi_m\left(\frac{z}{L}\right) - 1 \right] - \frac{g}{c_p}(z - z_0) & L > 0 \end{cases} \tag{17}$$

where z_0 corresponds to the roughness length of the site.

Based on measurements of the turbulent kinetic energy budget terms in the surface layer of an atmospheric boundary layer over a flat terrain [4], one can find:

$$\epsilon_0(z) = \frac{u_*^3}{Kz}\phi_\epsilon\left(\frac{z}{L}\right) \tag{18}$$

where

$$\phi_\epsilon\left(\frac{z}{L}\right) = \begin{cases} 1 - \dfrac{z}{L} & L < 0 \\ \phi_m\left(\dfrac{z}{L}\right) - \dfrac{z}{L} & L > 0 \end{cases} \tag{19}$$

Finally, making use of the k-ϵ model, a relation between turbulent kinetic energy k and ϵ is obtained:

$$k_0(z) = \sqrt{\frac{\mu_{t0}\epsilon_0}{\rho C_\mu}} = 5.48u_*^2\left[\frac{\phi_\epsilon\left(\dfrac{z}{L}\right)}{\phi_m\left(\dfrac{z}{L}\right)}\right]^{\frac{1}{2}} \tag{20}$$

where the constant 5.48 has been experimentally determined for the neutral atmospheric boundary layer [4].

The values of $C_\mu, C_{\epsilon 1}$, and $C_{\epsilon 3}$ must be changed from those in the original model proposed by Jones and Launder [10] (see Eq. (9)) to ensure that the basic-flow empirical expressions based on the Monin-Obukhov similarity theory (Eqs. (16)–(18) and (20)) represent an exact solution of the k-ϵ model. For instance, an expression for C_μ can be obtained by combining Eq. (20) with Eqs. (10) and (18):

$$C_\mu = 5.48^{-2} \tag{21}$$

An expression for $C_{\epsilon 1}$ can be obtained from the ϵ transport equation (Eq. (5)) by introducing the Monin-Obukhov empirical expressions for the case of neutral stratification (i.e., $L \to \infty$) [5,8]:

$$C_{\epsilon 1} = C_{\epsilon 2} - \frac{K^2}{\sqrt{C_\mu}\sigma_\epsilon} = 1.176 \tag{22}$$

These values of C_μ and $C_{\epsilon 1}$ have been proposed by Crespo et al. [5], along with a value of 0.8 for $C_{\epsilon 3}$. In the cases of stable and unstable stratification over a uniform flat terrain, the closure coefficients proposed by Crespo et al. [5] lead to inaccurate predictions (see Results section). It is important to note that while most of the closure coefficients in the k-ϵ model have values almost universally accepted, various values of $C_{\epsilon 3}$ have been proposed in the literature [11–13] ranging from −0.8 for unstable conditions up to 2.15 for stable conditions. Consequently, in an effort to improve the accuracy of the predictions in cases of stable and unstable stratification, the necessary condition on $C_{\epsilon 3}$ to ensure that the vertical distributions of k and ϵ given by Eqs. (18) and (20) are solutions of k-ϵ model has been obtained. This necessary condition on $C_{\epsilon 3}$ is constructed by first assuming that the Monin-Obuhkov distributions $[u_o(z), T_0(z), k_0(z)$ and $\epsilon_o(z)]$ are exact solution of the mathematical model (Eqs. (1)–(5)) when applied over a uniform flat terrain. Then, an expression for $C_{\epsilon 3}$ is obtained from the ϵ-equation (Eq. (5)):

Table 1 Coefficients for $C_{\epsilon 3}$

	$L>0$		$L<0$	
	$z/L<0.33$	$z/L>0.33$	$z/L<-0.25$	$z/L>-0.25$
a_0	4.181	5.225	−0.0609	1.765
a_1	33.994	−5.269	−33.672	17.1346
a_2	−442.398	5.115	−546.880	19.165
a_3	2368.12	−2.406	−3234.06	11.912
a_4	−6043.544	0.435	−9490.792	3.821
a_5	5970.776	0.000	−11163.202	0.492

$$C_{\epsilon 3} = 1 - \frac{\mu_{t0}\left(\dfrac{du_0(z)}{dz}\right)^2}{\beta g\dfrac{\mu_{t0}(z)}{\sigma_T}\left(\dfrac{dT_0(z)}{dz} + \dfrac{g}{c_p}\right)} + \frac{C_{\epsilon 2}\rho\epsilon_0(z)}{C_{\epsilon 1}\beta g\dfrac{\mu_{t0}(z)}{\sigma_T}\left(\dfrac{dT_0(z)}{dz} + \dfrac{g}{c_p}\right)} - \frac{k_0(z)}{\beta g\dfrac{\mu_{t0}(z)}{\sigma_T}\left(\dfrac{dT_0(z)}{dz} + \dfrac{g}{c_p}\right)\epsilon_0(z)C_{\epsilon 1}}\left[\frac{d}{dz}\left(\frac{\mu_{t0}}{\sigma_\epsilon}\frac{d\epsilon_0(z)}{dz}\right)\right] \tag{23}$$

Equation (23) was not amenable to a simple analytical form and a curve-fit expression has been derived:

$$C_{\epsilon 3}\left(\frac{z}{L}\right) = \sum_{n=0}^{5} a_n\left(\frac{z}{L}\right)^n \tag{24}$$

The coefficients of this series are shown in Table 1. On uniform flat terrain, these expressions are universal in the sense that they are the same for any values of L. However, they might not be appropriate over complex terrain. The resulting average value of $C_{\epsilon 3}$ under stable conditions is 3.4 and, under unstable conditions is −4.4.

3 Numerical Method

The complete set of fluid equations, expressed in a Cartesian coordinate system, consists of the continuity equation, three momentum equations for transport of velocity, the energy equation and the transport equations for k and ϵ. The solution of these equations is accomplished by employing FLUENT [14]. FLUENT uses a control-volume-based technique to convert the governing equations to algebraic equations that can be solved numerically. In this paper, the solution algorithm adopted is SIMPLEC [15]; the PRESTO (PREssure STaggering Option) interpolation scheme [14] is used for pressure and a second-order upwind scheme based on a multilinear reconstruction approach [16] is used for all other dependent properties.

3.1 Computational Domain. The atmospheric boundary layer over a flat terrain is two-dimensional. Thus, the computational domain consists of a simple rectangle. This domain is first discretized into quadrilateral elements defined by four nodes. Then, each element is considered as a control volume. All dependent variables are calculated at the centroid of the control volumes.

3.2 Boundary Conditions. Inlet boundary: The inlet boundary is a z line located upstream of the computational domain. The velocity field is prescribed by specifying $u_x = u_0(z)$ [see Eq. (16)] and $u_z = 0$ and the turbulent properties are set to the undisturbed flow conditions [see Eqs. (18) and (20)]. The pressure is calculated from the continuity equation. **Outlet boundary:** The outlet boundary is a z line located downstream of the computational domain. Here, the velocity field is calculated using the outflow treatment proposed by Patankar [17]. **Top boundary:** This bound-

ary is an x line where undisturbed flow conditions are prescribed for two velocity components and the turbulent properties, while pressure is calculated from the continuity equations. **Wall boundary:** The classical turbulent law of the wall is applied to the wall neighboring control volumes.

4 Results

This section aims to show the proposed method's ability to reproduce the properties of the atmospheric boundary layer for various thermal stability conditions on a flat terrain. The results presented in this section refer to simulations for three types of stratification, i.e., neutral, stable and unstable. These results are compared with the empirical solutions based on the Monin-Obukhov theory [4], and the numerical results obtained using the mathematical model proposed by Crespo et al. [5].

4.1 Description of the Problem. The problem solved in this section is a fully-developed turbulent boundary layer flow. Consequently, flow characteristics depend only on the vertical position, z, and not on the transverse position, y, and the longitudinal position, x, i.e., $u(z,L)$, $T(z,L)$, $k(z,L)$, and $\epsilon(z,L)$ where L corresponds to the Monin-Obukhov length.

Simulations were carried out for the three types of thermal stratification with a wind speed $u_0(H)$ and a turbulent intensity $TI(H)$ of 10 m/s and 8%, respectively, at a height H of 35 m. The physical properties of the air under standard conditions were prescribed, i.e., a density of 1.225 kg/m^3, a viscosity of $1.8*10^{-5}$ kg/m-s, and air specific heat of 1006.43J/kg K. Three Monin-Obukhov lengths were prescribed: $L=191$ m, $L\rightarrow\infty$, and $L=-231$ m, corresponding to stable, neutral, and unstable thermal conditions, respectively. These conditions were typical of those measured at the turbine hub height H in the wind park site of Alsvik [18,19]. The flow at the inlet of the computational domain was represented by imposing the empirical expressions based on the Monin-Obukhov theory for the velocity $u(z,L),T(z,L)$, turbulent kinetic energy $k(z,L)$, and $\epsilon(z,L)$. At the wall, the rough wall law was used with the following values:

- Neutral: with $z_0=0.00188$ m and a zero heat flux was fixed
- Stable: with $z_0=0.006$ m and a heat flux equal to -37.9 W/m^2 was fixed
- Unstable: with $z_0=0.0004$ m and a heat flux equal to 20.73 W/m^2 was fixed.

These values of z_0 and heat flux were computed from the Monin-Obukhov theory since the $u(H),TI(H)$, and L were prescribed.

It was found that a computational domain having a length of 425 m and a height of 180 m and discretized with a nonuniform grid composed of 18,000 control volumes was sufficient to guarantee a grid-independent solution. In this section, a rectangular computational domain composed of 18,000 elements was thus used to simulate the various conditions of thermal stratification. The height of the computational domain was discretized using 110 grid points. The grid size in the vertical direction was varied from 0.6 m (near the ground) to 5.6 m (at the top of the computational domain).

The solution to a similar problem was obtained by Crespo et al. [5]. Their mathematical model was very similar to the one used in this paper, it was based on the solution of the Navier-Stokes equations, coupled with a k-ϵ turbulence model modified for the neutral atmospheric boundary layer. Comparisons between the empirical solutions based on the theory of Monin-Obukhov and these numerical solutions are presented in Figs. 1–4 for neutral, stable, and unstable thermal stratification to better illustrate the effects of thermal stratification on the atmospheric boundary layer, profiles for velocity, temperature, turbulent kinetic energy, and turbulent rate of dissipation on a flat terrain. At a height of 35 m, the same velocity (10 m/s) and turbulent intensity (8%) were prescribed for the three types of stratification. Depending on the stability of the atmosphere, significant differences between the vertical distributions were observed. These are particularly significant for the vertical distribution of the velocity under stable conditions and the vertical distribution of the turbulent kinetic energy under unstable conditions. Also included in Figs. 1–3 are experimental data taken from the Co-operative Atmosphere-Surface Exchange Study 1999 (CASES99). We can see a very good agreement between the Monin-Obukhov theory and the measurements for the velocity and temperature profiles. The turbulence intensity profiles do not show agreement.

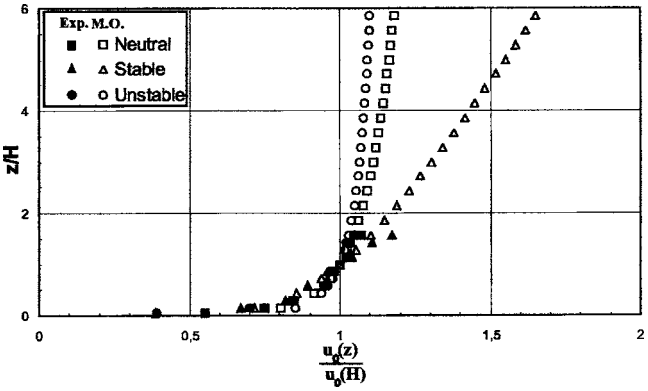

Fig. 1 Velocity profiles on a flat terrain with $H=35$ m, $u_0(H)=10$ m/s, and $TI(H)=8\%$

4.2 Neutral Conditions. These conditions of stratification are rare and are considered ideal. They correspond to weather condi-

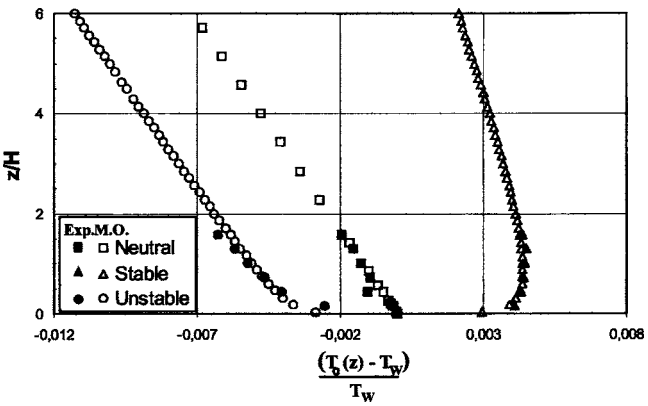

Fig. 2 Temperature profiles on a flat terrain with $H=35$ m, $u_0(H)=10$ m/s, and $TI(H)=8\%$

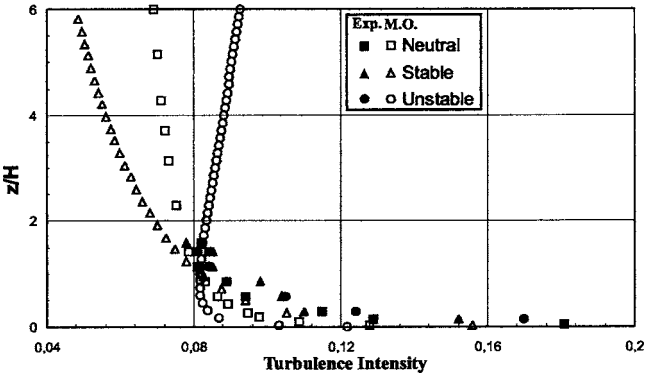

Fig. 3 Turbulent intensity profiles on a flat terrain with $H=35$ m, $u_0(H)=10$ m/s, and $TI(H)=8\%$

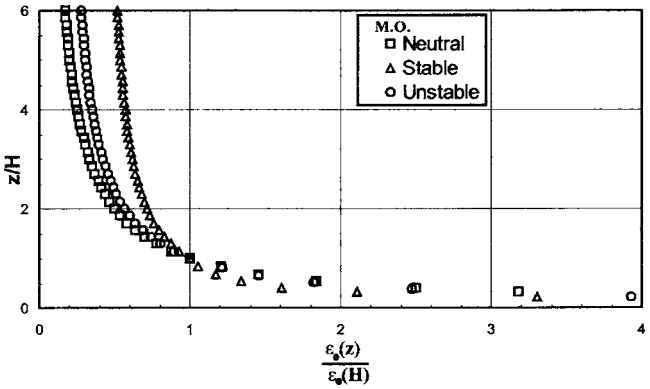

Fig. 4 Turbulent dissipation profiles on a flat terrain with H =35 m, $u_0(H)$=10 m/s, and $TI(H)$=8%

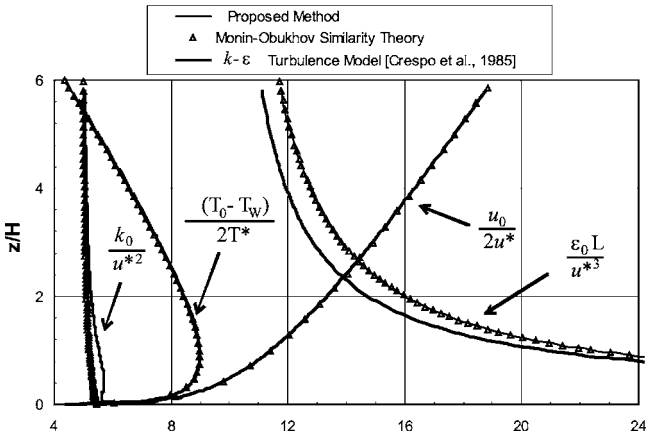

Fig. 6 Stable atmospheric boundary layer with H=35 m, $u_0(H)$=10 m/s, $TI(H)$=8%, z_0=6 mm, and L=191 m

tions at the end of the day, or when wind speeds are high. Under such conditions, the origin of atmospheric turbulence is mainly mechanical, i.e., turbulence results only from the friction of the ground and shearing in the velocity field.

The results presented in this section include a comparison between the results obtained using the original Jones-Launder k-ϵ model [10] (i.e., C_μ=0.09 and $C_{\epsilon 1}$=1.44), the Crespo et al. model and the proposed k-ϵ model–all implemented in FLUENT—and the empirical solutions given by the Monin-Obukhov theory. Figure 5 presents the comparison of these results. The modifications introduced for the turbulence model, under these neutral conditions, are the same as those proposed by Crespo et al. [5] (i.e., C_μ =0.0333 and $C_{\epsilon 1}$=1.1764). Consequently, the results of the simulations using the proposed model are identical the those of the Crespo et al. model. The results show significant differences between the empirical expressions and the Jones-Launder simulations, mainly for the values of the turbulent kinetic energy k and the dissipation rate of turbulent kinetic energy ϵ. These differences arise from the fact that the empirical distributions for the velocity, temperature and turbulent properties k and ϵ, representing the atmospheric boundary layer, are not solutions of the original Jones-Launder k-ϵ model. Figure 5 also includes the results obtained using the k-ϵ model proposed in this paper. The simulations obtained using this method correlate very well with the empirical expressions.

4.3 Stable Conditions. These conditions of stratification correspond to night-time weather conditions, when the temperature at ground level is lower than that of the ambient air. Under such conditions, atmospheric turbulence results from the forces of friction and shearing, as well as from thermal stratification of the air. The effects of the buoyancy forces then contribute to decreasing the turbulent kinetic energy in the terrestrial boundary layer.

Figure 6 presents the solutions of the dependent variables, u, k, and ϵ for a stable atmospheric boundary layer by using the constants recommended by Crespo et al. [5]. The results show that the value of $C_{\epsilon 3}$ given by Crespo et al. produces significant differences between the simulations and empirical expressions, in particular for the values of k and ϵ. These differences are due to the fact that the empirical distributions of the velocity, temperature and turbulent properties k and ϵ, representing the atmospheric boundary layer, are not solutions of the k-ϵ model suggested by Crespo et al. [5]. Also included in Fig. 6 are the results obtained using the k-ϵ model proposed in this paper. Figure 6 clearly illustrates the improvement in simulation accuracy with respect to the Monin-Obukov empirical expressions when using the proposed method instead of the model proposed by Crespo et al. [5].

4.4 Unstable Conditions. These stratification conditions correspond to daytime weather conditions, when the temperature at ground level is higher than that of the ambient air. Under such conditions, atmospheric turbulence arises from the forces of friction and shearing, as well as from thermal stratification of the air. The effects of the buoyancy forces then help reinforce exchanges of air and increase the turbulent kinetic energy in the atmospheric boundary layer.

Figure 7 presents the solutions for the dependent variables, u, k,

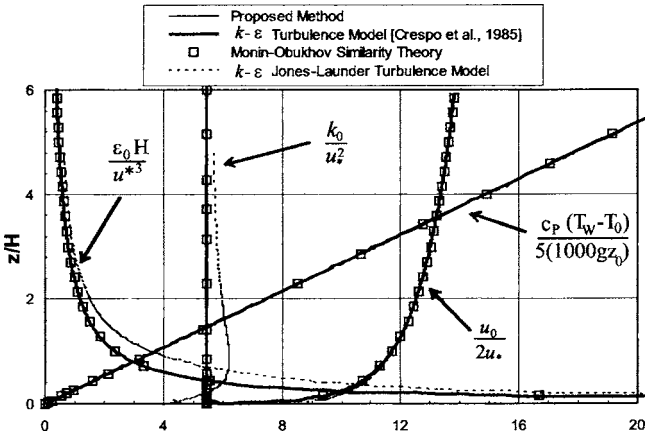

Fig. 5 Neutral atmospheric boundary layer with H=35 m, $u_0(H)$=10 m/s, $TI(H)$=8%, z_0=1.88 mm, and $L \rightarrow \infty$

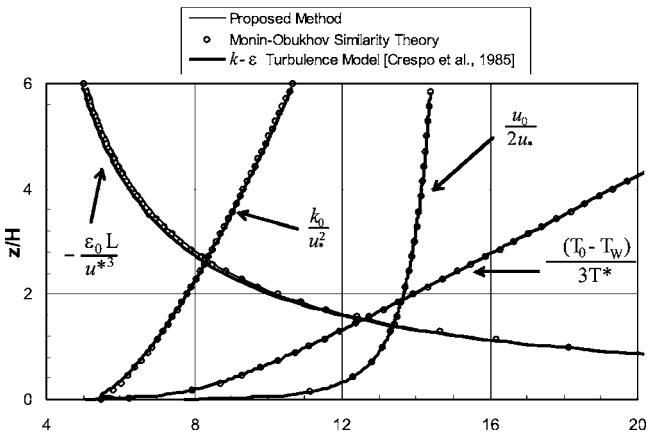

Fig. 7 Unstable atmospheric boundary layer with H=35 m, $u_0(H)$=10 m/s, $TI(H)$=8%, z_0=0.4 mm, and L=–231 m

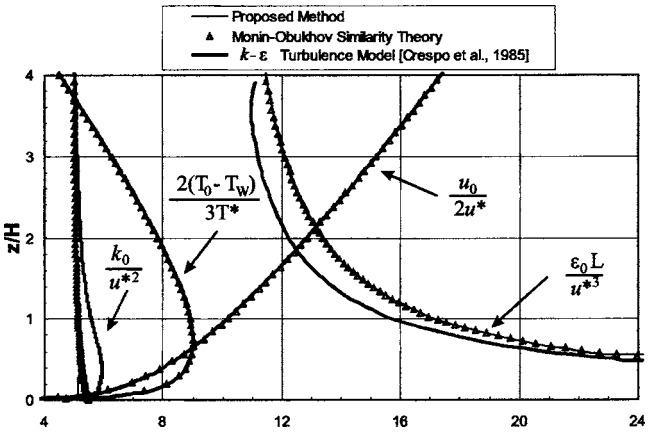

Fig. 8 Stable atmospheric boundary layer with H=55 m, $u_0(H)$=9 m/s, $TI(H)$=9%, z_0=50 mm, and L=177 m

and ϵ for an unstable atmospheric boundary layer, using the constants suggested by Crespo et al. [5]. The results show once again that the value of $C_{\epsilon 3}$ proposed by Crespo et al. induces only minor differences between the simulations and the empirical expressions, in particular for the values of ϵ. The results obtained with the mathematical model proposed in this paper, also shown in Fig. 7, do not show any significant improvement.

4.5 Demonstration of the Validity of the Expression for $C_{\epsilon 3}$. To illustrate the validity of the expression for $C_{\epsilon 3}$ as a function of L, an atmospheric boundary layer having the following characteristics was also analyzed:

- wind speed at 9 m/s and a turbulent intensity of 9% at a height H of 55 m
- Stable: with L=177 m, z_0=0.05 m and a heat flux equal to −41.9 w/m^2 was fixed
- Unstable: with L=−121 m, z_0=0.0004 m and a heat flux equal to 28.4 W/m^2 was fixed.

Figures 8 and 9 show the results for stable and unstable situations, respectively. The results obtained using the proposed k-ϵ model are again in very good agreement with the empirical solutions provided by the Monin-Obukhov theory; they agree better than the Crespo et al. results for stable conditions, and differ by about the same amount as the Crespo et al. results for unstable conditions.

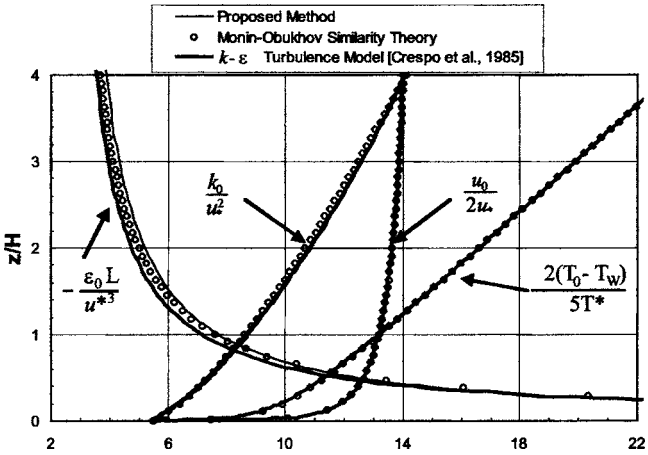

Fig. 9 Unstable atmospheric boundary layer with H=55 m, $u_0(H)$=9 m/s, $TI(H)$=9%, z_0=0.4 mm, and L=−121 m

5 Conclusion

The main purpose of this paper is to numerically predict the effects of thermal stratification of the atmospheric boundary layer. The flow field is described by the Reynolds' averaged Navier-Stokes equations, complemented by the k-ϵ turbulence model. An original expression for the closure coefficient related to the buoyancy production term is proposed in an effort to improve the accuracy of the simulations. This new expression has made a significant improvement in the accuracy of simulations under stable conditions. For unstable stratifications, the improvement in accuracy is not significant.

Acknowledgments

This study has received support from the Canada Research Chair Program, the *Ministère des ressources naturelles du Québec* through the *Programme d'aide au développement des technologies de l'énergie*, and the Canadian Natural Resources Ministry through the Efficiency and Alternative Energy Program. Support from the Natural Sciences and Engineering Research Council of Canada (NSERC) in the form of research grants is gratefully acknowledged.

References

[1] Högström, U., Asimakopoulos, D. N., Kambezidis, H., Helmis, C. G., and Smedman, A., 1988, "A Field Study of the Wake behind a 2 MW Wind Turbine," Atmos. Environ., **22** (4), pp. 803–820.
[2] Vermeer, L. J., Sorensen, J. N., and Crespo, A., 2003, "Wind Turbine Wake Aerodynamics," Prog. Aerosp. Sci., **39**, pp. 467–510.
[3] Gibson, M. M., and Launder, B. E., 1976, "On the Calculation of Horizontal, Turbulent, Free Shear Flows Under Gravitational Influence," ASME J. Heat Transfer, **98**(1), pp. 81–87.
[4] Panofsky, H., Dutton, and J., 1984, *Atmospheric Turbulence*, Wiley, New York.
[5] Crespo, A., Manuel, F., Moreno, D., Fraga, E., and Hernandez, J., 1985, "Numerical Analysis of Wind Turbine Wakes," *Workshop on Wind Energy Applications, Delphi, Greece*.
[6] Riddle, A., Carruthers, D., Sharpe, A., McHugh, C., and Stocker, J., 2004, "Comparison between FLUENT and ADMS for Atmospheric Dispersion modeling," Atmos. Environ., **38**, pp.1029–1038.
[7] Thanh, C. V., Yasunobu, A., and Takashi, A., 2002, "A k-ϵ Turbulence Closure Model for the Atmospheric Boundary Layer Including Urban Canopy," Boundary-Layer Meteorol., **102**, pp. 459–490.
[8] Apsley, D. D., and Castro, I. P., 1997, "A Limited-Length-Scale k-ϵ Model for Neutral and Stably-Stratified Atmospheric Boundary Layer," Boundary-Layer Meteorol., **83**, pp. 75–98.
[9] Mellor, G. L., and Yamada, T., 1982, "Development of a Turbulence Closure Model for Geophysical Fluid Problems," Rev. Geophys. Space Phys., **20**, pp. 851–875.
[10] Jones, W. P., and Launder, B. E., 1972, "The Prediction of Laminarization with a Two-Equation Model of Turbulence," Int. J. Heat Mass Transfer, **15**, pp. 301–314.
[11] Rodi, W., 1982, *Turbulent Buoyant Jets and Plumes*, Pergamon Press, New York, p.184.
[12] Kitada, T., 1987, "Turbulence Structure of Sea Breeze Front and its Implication in Air Pollution Transport-Application of k-ϵ Turbulence Model," Boundary-Layer Meteorol., **41**, pp. 217–239.
[13] Betts, P. L., and Haroutunian, V., 1983, "A k-ϵ Finite Element Simulation of Buoyancy Effects in the Atmospheric Surface Layer," ASME paper 83-WA/HT-32.
[14] *FLUENT 6 User's Guide*, 2001, Volume 1-4, Fluent Inc., Lebanon.
[15] Vandoormaal, J. P., and Raithby, G. D., 1984, "Enhancements of the SIMPLE Method for Predicting Incompressible Fluid Flows," Numer. Heat Transfer, **7**, pp. 147–163.
[16] Barth, T. J., and Jespersen, D., 1989, "The Design and Application of Upwind Schemes on Unstructured meshes, AIAA paper AIAA-89-0366, *AIAA 27th Aerospace Sciences Meeting, Reno, NV*.
[17] Patankar, S. V., 1980, *Numerical Heat Transfer and Fluid Flow*, McGraw-Hill, New York.
[18] Magnusson, M., and Smedman, A.-S., 1994, "Influence of Atmospheric Stability on Wind Turbine Wakes," Wind Eng., **18**(3), pp. 139–152.
[19] Magnusson, M., and Smedman, A.-S., 1999, "Air Flow behind Wind Turbines," J. Wind. Eng. Ind. Aerodyn., **80**(1-2), pp. 169–189.